N91-10465

Multi-spectral Window Radiance Observations of Cirrus from Satellite and Aircraft - November 2, 1986 "Project FIRE"

W. L. Smith, H. E. Revercomb, H. B. Howell, and M.-X. Lin[1]

Cooperative Institute for Meteorological Satellite Studies
University of Wisconsin-Madison
Madison, Wisconsin

[1]State Meteorological Administration
National Meteorological Bureau
Beijing, China

Abstract

High resolution infrared radiance spectra achieved from the NASA ER2 airborne HIS experiment are used to analyze the spectral emissivity properties of CIRRUS cloud within the 8-12μm atmospheric "window" region. Observations show that the cirrus emissivity generally decreases with increasing wavenumber (i.e., decreasing wavelength) within this band. A very abrupt decrease in emissivity (increase in brightness temperature) exists between 930 cm^{-1} (10.8μm) and 1000 cm^{-1} (10.0μm), the magnitude of the change being associated with the cirrus optical thickness as observed by lidar. The HIS observations are consistent with theoretical calculations of the spectral absorption coefficient for ice.

The HIS observations imply that cirrus cloud can be detected unambiguously from the difference in brightness temperatures observed within the 8.2μm and 11.0μm window regions of the HIRS sounding radiometer flying on the operational NOAA satellites. This ability is demonstrated using simultaneous 25 km resolution HIRS observations and 1 km resolution AVHRR imagery achieved from the NOAA-9 satellite. Finally, the cirrus cloud location estimates combined with 6.7μm channel moisture imagery portray the boundaries of the ice/vapor phase of the upper troposphere moisture. This phase distinction is crucial for infrared radiative transfer considerations for weather and climate models, since upper tropospheric water vapor has little effect on the earth's outgoing radiation whereas cirrus cloud has a very large attenuating effect.

1. Importance of Cirrus Detection

The detection of cirrus clouds from satellites is important for at least two reasons: (1) the monitoring of long-term changes of cloud cover, since cirrus variability greatly impacts the greenhouse effect, and (2) the elimination of infrared radiances observed by sounding radiometers effected by cloud prior to the temperature profile retrieval process since undetected cirrus cloud contamination leads to a systematic cold bias in the result.

2. Prior Work

Several authors have addressed the optically thin cirrus detection problems (Prabahkara, 1987; Inoue, 1985, Wu, 1987). Smith et al. (1969), Arking (1985), and Wu (1987) point out that thin cirrus cloud can be detected by the difference in brightness temperature observed in the 3.8μm and 11μm window regions because of the different Planck radiant energy dependence upon temperature at these two wavelengths. When viewing through thin cirrus, the measured radiance is a function of both the cold cloud and warm surface temperatures. Because of the higher ordered dependence of radiance upon temperature at 3.8μm, the 11μm brightness temperature will be observed to be lower than the 3.8μm brightness temperature in the presence of thin cirrus. However, this relationship is not unique in that similar differences occur during the daytime due to differential reflected sunlight contributions to the two channels and for broken middle or low clouds due to the differential Planck effect. More recently, Inoue (1985) and Prabahkara (1987) pointed out that the absorption for ice is larger at 12μm than at 11μm so that the "split window" difference (i.e., the difference in brightness temperatures observed in the 11μm and 12μm channels of the Advanced Very High Resolution Radiometer (AVHRR) flying aboard the operational NOAA satellites) can be used to detect thin cirrus cloud. However, this differential relation is not unique either, since water vapor absorption can produce a similar effect.

3. HIS Observations

Most recently, spectral radiometric observations of cirrus clouds were achieved during the First ISCCP Regional Experiment (FIRE) conducted over southcentral Wisconsin during October-November 1986. The observations were conducted with the High resolution Interferometer Sounder (HIS) flying aboard the NASA ER2 aircraft. Here we discuss the cirrus observed over Wisconsin on November 2, 1986. As shown in the Fig. 1 example, the HIS spectral radiances reveal an increase in cirrus cloud absorption and emissivity (decrease in radiating brightness temperature) across the 10-12μm window region with a very sharp increase taking place between 10 and 11μm (i.e., 1000-900 cm^{-1}). HIS observations between 8 and 10μm (not shown) reveal no significant change in cirrus emissivity between 8 and 10μm. The HIS observations are in good agreement with theoretical calculations of ice absorption by Irvine and Pollack (1968) as shown in Fig. 2. (Figures 4 and 5 show satellite images of the cirrus observed from the ER2.)

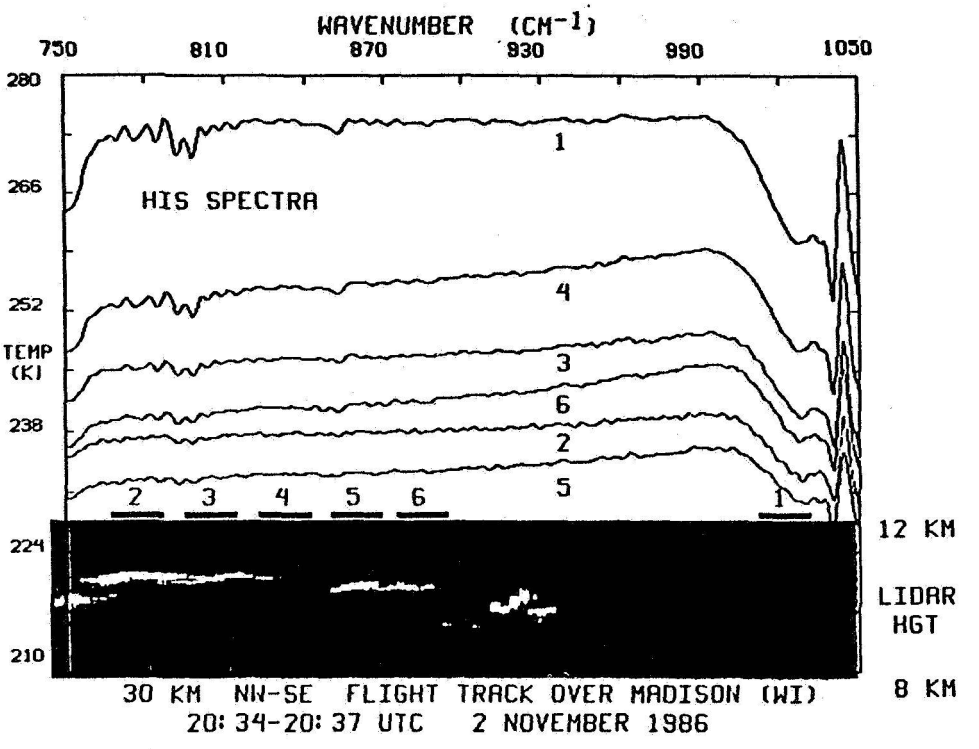

Fig. 1. A set of 10-12μm "window" region cirrus cloud brightness temperature spectral observed from the NASA ER2 on November 2, 1986 near Madison, Wisconsin. Also shown is an image of the cirrus cloud backscatter between 8 and 12 km (no significant return outside this altitude range) of light pulses from a lidar (Spinherne, 1982) also aboard the ER2. The field of view of the HIS corresponding to each spectrum is shown above the lidar.

4. Application to Satellite Observations

Because water vapor absorption is generally larger in the 8-9μm window region than within the 11-12μm region, a positive brightness temperature difference between these two window regions is a definite indicator of the presence of cirrus cloud. This principal is demonstrated using the 8.2 and 11.1μm channel observations of the High Resolution Infrared Radiation Sounder (HIRS) radiometer flying aboard the polar orbiting NOAA satellites.

Figure 2 shows the spectral response of the HIRS 11.1μm (H8) and 8.2μm (H10) channels relative to the volume absorption coefficient for ice. As can be seen, there should be a significant difference

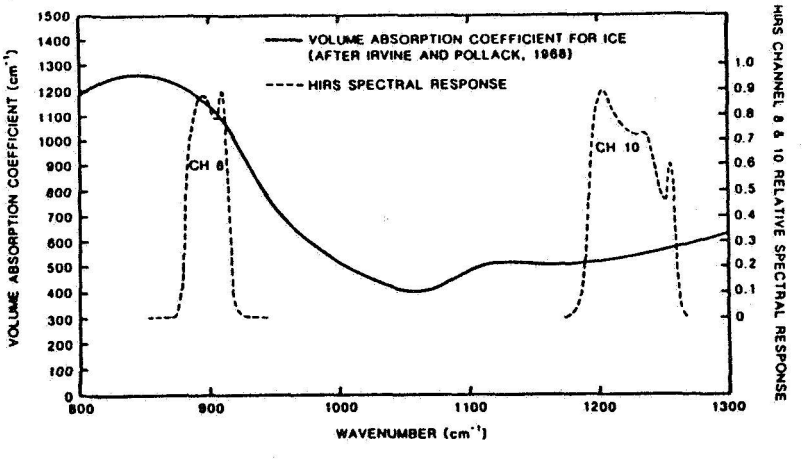

Fig. 2. Volume absorption coefficient for ice and the spectral response of HIRS channels 8 and 10.

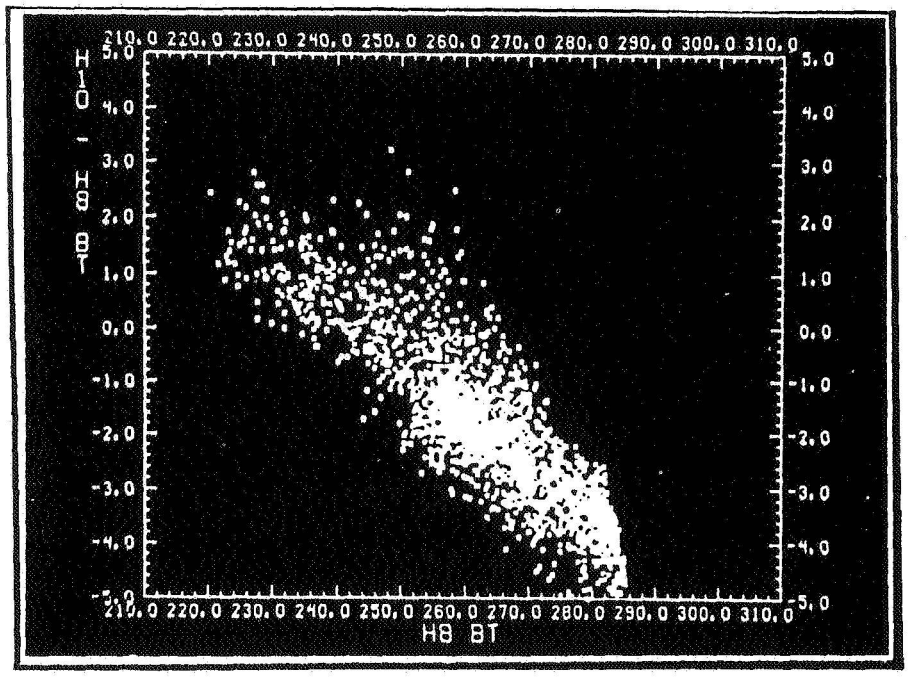

Fig. 3. Scatter diagram of the difference in brightness temperature observed in the HIRS 8.2μm (H10) and 11.1μm (H8) channels as a function of 11.1μm (H8) brightness temperature. Positive differences indicate the presence of semi-transparent cirrus cloud.

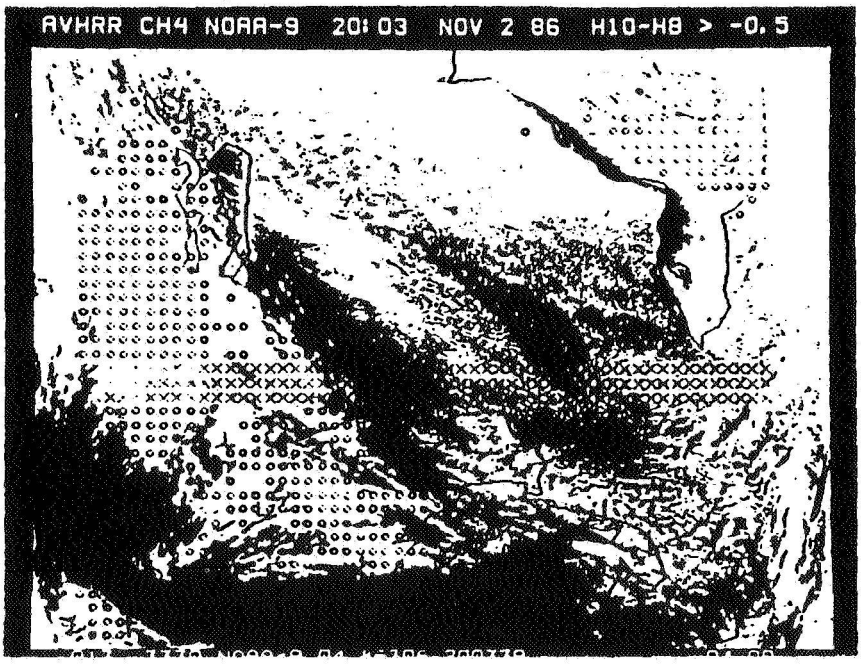

Fig. 4. An image of cloud cover at 20 GMT on November 2, 1986 as observed by the AVHRR 11μm channel (Ch4). Superimposed are circles delineating areas of cirrus cloud detected from the HIRS 8.2 and 11.1μm window channel differences. The crosses denote the gap in earth coverage due to instrumental calibration.

in the brightness temperature observed by these two channels when viewing semi-transparent cirrus cloud. Figure 3 shows a scatter diagram of the difference in brightness temperature observed in the HIRS 8.2μm channel (H10) and the HIRS 11.1μm channel (H8) as a function of the 11.1μm brightness temperature observation over the upper midwest on November 2, 1986 (see Fig. 4). As shown, most of the observations are free of cirrus clouds as indicated by the negative differences. Apparent cirrus cloud conditions, however, do cover a wide range of optical thicknesses as indicated by the wide range

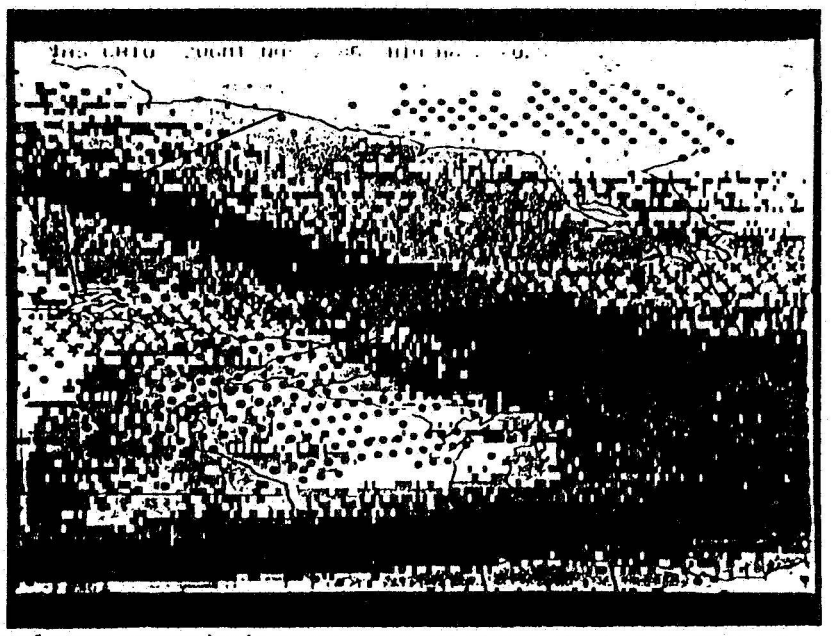

Fig. 5. An image of upper tropospheric water vapor and cirrus cloud at 20 GMT on November 2, 1986 as observed by the GOES-VAS 6.7μm H_2O absorption channel. As in Fig. 4, the circles show regions of cirrus as detected from the NOAA-HIRS 8.2μm and 11.1μm brightness temperature difference.

of 11.1μm brightness temperature observations (220-268°K) associated with positive indications of cirrus clouds (i.e., plus H10-H8 brightness temperature differences). Assuming a mean surface skin temperature of 280°K and a probable cirrus cloud temperature of 220°K, the temperature at the 10 km cirrus height depicted by lidar (Fig. 1), the cirrus optical thickness for the 11.1μm channel is as low as 0.2, indicating that cirrus with transmissivities as high as 80% were detected by the HIRS in this case.

Figure 4 shows the location (denote by circles) of HIRS detected cirrus superimposed upon an AVHRR infrared image. Because the instrumental noise of the HIRS is about 0.25°K for typical cloud temperatures, a threshold of -0.5°K for the difference was used to discriminate cirrus contaminated HIRS fields-of-view. The circles depict the geographical dimension of the 25 km HIRS field-of-view. Based on comparison with the cloud morphology in the AVHRR image, the objective cirrus detection technique seems to work very well, except when the cirrus occupies only a small portion of the HIRS field-of-view.

5. Water Phase Detection

The combination of 6.7μm, 8.2μm, and 11.1μm brightness temperature data can be used to differentiate between upper level moisture in the vapor phase from that which has sublimated into the ice phase. This distinction is very important with regard to the analysis of the "greenhouse effect" on the earth's climate since upper level water vapor is largely transparent to the outgoing radiation to space whereas cirrus cloud produces a very large decrease in the radiation to space.

Upper tropospheric moisture imagery, obtained from 6.7μm geostationary satellite measurements is routinely used for the depiction of large scale weather patterns. It would be extremely useful to have an 8.2μm channel as part of the geostationary imagery system so that the phase of the upper level moisture depicted by the 6.7μm channel could be diagnosed. An example of the results which could be achieved is generated by superimposing HIRS cirrus cloud depictions over a GOES-VAS 6.7μm moisture image obtained at nearly the same time. Figure 5 shows the result. If one had a time sequence of such inferences, the phase change process could be observed, thus providing important measurements of upper tropospheric cloud dynamics as well as the upper tropospheric radiative properties important for weather and climate analyses.

6. Additional Considerations

It is worth noting that cirrus cloud microphysical properties (e.g., partical size distribution) might be deduced from the high resolution HIS spectra and the simultaneous lidar observations conducted from the ER2 aircraft (an example of which is shown in Fig. 1). The optical thickness, τ, of the cloud for "window" wavelengths in between gaseous absorption lines can be shown to be given by

$$\tau_\nu = B_\nu \Delta Z = -\ln \left[\frac{I_\nu - B_\nu (T_{cd})}{B_\nu(T_s) - B_\nu (T_{cd})} \right] \qquad (1)$$

where β_ν is the absorption coefficient, ΔZ the geometrical thickness, I_ν is the observed radiance, T_s and T_{cd} are the surface and cloud temperature, respectively, and B is the Planck radiance. The surface skin temperature T_s can be observed from neighboring cloud-free fields-of-view and T_{cd} is taken from a clear sky temperature profile at the cloud altitude depicted by the lidar. The geometric thickness of the cloud ΔZ is also provided by the lidar for optically thin cloud (see Fig. 1). Consequently, the combination of HIS and lidar observations provides a measure of the infrared absorption coefficient spectrum for the cloud. The absorption coefficient is related to the cloud particle properties through the relation

$$\beta_\nu = K(\eta_i \eta_r)\ \nu \int_0^\infty r^3\, N(r)\, dr \qquad (2)$$

where $K(\eta_i, \eta_r)$ is a function of the imaginary and real parts of the index refraction for ice, r is the radius of the ice particles (assumed to be effective spheres) and N(r) is the size distribution. If it is assumed that the size distribution can be expressed as a linear combination of Gaussian distributions, i.e.,

$$N(r) = \sum_{i=1} n[r_i(o)] \exp\left\{ \sqrt{\frac{[r - r_i(o)]^2}{2\sigma_i^2}} \right\}, \qquad (3)$$

then estimates of the size distribution might be obtained by solving for those $r_i(o)$ and σ_i values which best satisfy the observed absorption coefficient spectra. This research is the subject of a future paper.

Acknowledgments

We thank H. Woolf of CIMSS for his assistance with the HIS data reduction. J. Spinhirne (NASA/GSFC) graciously provided the ER2 lidar data. Special thanks go to the flight crew of the NASA ER2 for their flawless performance of their difficult mission. L. Beckett and G. Wade are gratefully acknowledged for their help in preparing this manuscript. This research was supported by NASA Contract NAS1-18277.

References

Smith, W. L., 1969: The improvement of clear column radiance determination with a supplementary 3.8μm window channel. ESSA Technical Memorandum NESCTM 16, 17 pp.

Spinherne, J. D., M. Z. Hansen, and L. O. Caudill, 1982: Cloud top remote sensing by airborne lidar. Appl. Optics, 21, 1564-1571.

Arking, A., and J. D. Childs, 1985: Retrieval of cloud cover parameters from multispectral satellite images. J. Clim. Appl. Meteor., 24, 322-333.

Inoue, T., 1985: On the temperature and effective emissivity determinations of semi-transparent cirrus clouds by bi-spectral measurements in the 10um window region. J. Meteor. Soc. Japan, 63, 88-89.

Wu, M.-L. C., 1987: A method for remote sensing the emissivity, fractional cloud cover, and cloud top temperature of high level, thin clouds. J. Clim. Appl. Meteor., 26, 225-233.

Prahahkara, C. P., R. S. Fraser, G. Delu, M.-L. C. Wu, R. J. Curran, and T. L. Styles, 1987: Thin cirrus clouds: seasonal distribution over oceans deduced from Nimbus 4 IRIS. J. Clim. Appl. Meteor.